Available online at www.sciencedirect.com
SCIENCE DIRECT
Polymer 46 (2005) 129–136
polymer
www.elsevier.com/locate/polymer

New fabricate of styrene–butadiene rubber/montmorillonite nanocomposites by anionic polymerization

Zhenjun Zhang[a,c], Lina Zhang[a,b,*], Yang Li[c], Hongde Xu[c]

[a]*Department of Chemistry, Wuhan University, Wuhan 430072, China*
[b]*Center of Nanoscience and Nanotechnology, Wuhan University, Wuhan 430072, China*
[c]*Research Institute of Beijing Yanshan Petrochemical Co. Ltd, Beijing 102500, China*

Received 3 August 2004; received in revised form 24 October 2004; accepted 8 November 2004
Available online 24 November 2004

Abstract

Styrene–butadiene rubber/montmorillonite (SBR/MMT) nanocomposites were successfully synthesized by in situ living anionic polymerization with *n*-BuLi as initiator. The results from kinetics study and ^{1}H NMR indicated that the addition of organophilic montmorillonite (OMMT) did not changed the living copolymerization and the components of the copolymer on the whole when OMMT content was lower than 3 wt %. However, gel permeation chromatography showed that the introduction of OMMT resulted in small amount of high-molecular weight fraction of SBR in the composites, leading to an increase in the weight-average molecular weight and polydispersity index, but the unchangeableness of the number-average molecular weight. The result from transmission electron microscopy and X-ray diffraction revealed that a completely exfoliated structure existed in the nanocomposite with 25 wt % styrene and OMMT content from 1 to 4 wt %, and styrene played an important role in the expanding of OMMT layers. Moreover, the nanocomposites possessed higher glass-transition temperature, thermal stability, tensile strength and elongation at break than SBR when the OMMT content ranged from 2.5 to 4 wt %. A schema was proposed to illustrate the formation of the nanocomposite and the exfoliation structure with physical cross-linking between SBR chains and OMMT.

Keywords: Nanocomposites; Styrene–butadiene rubber; Montmorillonite

1. Introduction

Now-a-days, nanomaterials have attracted much attention, and clays have been extensively used for preparation of nanocomposites. As a result of the large interfacial area per unit volume, polymer–clay nanocomposites possess unique properties that are not shared by conventional composites [1], such as excellent mechanical properties [2,3], high thermal stability [4,5], improved barrier properties [6,7] and flame retardance [8]. According to the degree of dispersion the polymer/clay composites can be divided into three types. The first type is conventional composites containing clay tactoids, in which the clay tactoids are dispersed simply as a segregated phase. The second one is intercalated polymer–clay nanocomposites, where silicate sheets maintain their layered stacking, but polymer chains insert into the clay host gallery. The last one is the exfoliated polymer–clay nanocomposites, in which individual silicate sheets lose their layered geometry, and are dispersed in the polymers at the nanoscale, accompanied with a very large polymer/filler interface, resulting in excellent physical properties [9,10]. Though a lot of organoclay-thermoplastics have been prepared and studied [11–14], less attention has been paid to use organically modified layered silicates in reinforcing elastomers [15,16].

Styrene–butadiene rubber (SBR) is a random copolymer of styrene and butadiene. To improve properties of polymer/clay nanocomposites, montmorillonite (MMT) is probably the most suited material [17–22]. It has been reported [23] that SBR and organophilic montmorillonite (OMMT) were directly mixed to obtain nanocomposites, which have showed intercalated and partly exfoliated

* Corresponding author. Tel.: +86 278 721 9274; fax: +86-27-68756661.
E-mail address: lnzhang@public.wh.hb.cn (L. Zhang).

0032-3861/$ - see front matter © 2004 Elsevier Ltd. All rights reserved.
doi:10.1016/j.polymer.2004.11.008

structure with improved viscoelastic and mechanical properties. However, a completely exfoliated SBR/MMT nanocomposite prepared by living anionic polymerization has been never reported in literatures. It is noted that living polymerization provides the best methodology for the synthesis of polymers with predictable molecular weights and narrow distributions of molecular weight. Using this method with the living nature of propagating chain-ends, it is also possible to design and synthesize well-defined block copolymers as well as specially shaped polymers with precise molecular architectures such as chain-end- and in-chain-functionalized polymers, cyclic, star-shaped, comb-like, graft and hyperbranched polymers [24]. In this paper, exfoliated SBR/MMT nanocomposite by living anionic polymerization was prepared. The effects of styrene and OMMT content on the exfoliation of OMMT layers, copolymerization reaction, as well as the structure and properties of the nanocomposites were studied by transmission electron microscopy, X-ray diffraction, ^{1}H NMR, differential scanning calorimetry, thermogravimetric analysis and tensile testing.

2. Experimental section

2.1. Materials

OMMT (NANNOLIN DK4) was supplied by Fenghong Clay Chemical Corporation in China. The clay was exchanged by a quaternary long organic ammonium salt with cation exchange capacity of 110 meq/100 g to obtain an average particle size of 25×1000 nm in the dry state. All materials used were purified before use. Styrene (Yanshan Petrochem. Co., China, polymerization grade) was treated with activate alumina to remove the inhibitor and deoxygenated. Butadiene (Yanshan Petrochem. Co., China, polymerization grade) was treated with minor *N*-butyllithium (*n*-BuLi) to remove moisture and inhibitor. Cyclohexane (Jinxi Chemical Plant, China, chemical grade) was dried with 5-Å molecular sieves and deoxygenated. *n*-BuLi was self-made, and its concentration was calibrated by Gilman double titration method [25]. Tetrahydrofuran (THF, Beijing Yili Fineness Chemical Factory, China) was analytical grade, and was refluxed over CaH_2 for more than 4 h and then distilled.

2.2. Synthesis of SBR/MMT nanocomposites

A given amount of styrene, butadiene, THF (THF: *n*-BuLi = 25), OMMT and cyclohexane were introduced into a 5 L polymerization kettle filled with purified N_2. After stirring for 3 h, a little *n*-BuLi was added to remove impurities in the system, and then a stoichiometric amount (according to a designed molecular weight of 1.5×10^5) of *n*-BuLi as initiator was added into the kettle. The polymerization was carried out at 50 °C for 3 h to obtain SBR/MMT nanocomposite. Absolute ethyl alcohol was used as terminating agent. The resultant product was vacuum-dried for 24 h at 80 °C. By setting the OMMT content to be 3 wt % and changing the monomer ratio of styrene to butadiene (such as 0:100, 10:90, 25:75, 40:60, 60:40 and 100:0), a series of the polymers/MMT products were prepared, and coded as S-0M3, S-10M3, S-25M3, S-40M3, S-60M3 and S-100M3, respectively. Using the ratio of styrene to butadiene (25:75), SBR/MMT nanocomposites containing 0, 1, 2, 2.5, 3 and 4 wt % OMMT were prepared, and coded as SB, S-25M1, S-25M2, S-25M2.5, S-25M3 and S-25M4, respectively. In addition, to measure the mechanical properties of the SBR/MMT nanocomposites a mixture containing 100 g of SBR/MMT or SB, 3 phr of zinc oxide, 1.7 phr of sulfur, 2 phr of stearic acid, 1 phr of cyclohexyl benzothiazole sulfenamide (CBS), 45 phr of carbon black, was vulcanized at 145 °C for 30 min to obtain the vulcanized sheets.

2.3. Characterization

The residual monomers in the polymerization mixture were analyzed with gas chromatography (GC, SHIMADZU GC-14A, Japan). An AC-1 column (60 m×0.25 mm I.D. with a thickness of 0.5 μm) was used. The carrier gas was nitrogen (99.999%) at a flow rate of 1.5 mL/min. An initial temperature for GC was 40 °C, followed by increasing the temperature at a rate of 10 °C/min to 120 °C for 10 min.

The molecular weights and molecular weight distributions of the SBR copolymers were measured with a gel permeation chromatography (GPC, SHIMADZU 10A, Japan) equipped with three columns of TSK-GEL multipore HXL-M (7.8 mm×300 cm) at room temperature. The eluent was THF. The samples were dissolved in THF overnight to prepare transparent solution with 1.0 mg/mL concentration. The THF and polymer solution were filtered with a 0.45 μm filter to remove clays and then degassed before use. The injection volume was 100 μL for each sample, and the flow rate was 1.0 mL/min. The calibration curves for GPC were obtained by using TSK standard samples of polystyrene (Japan). Class-LC10 software was utilized for data acquisition and analysis.

The X-ray diffraction measurement of the samples was carried out on an X-ray diffractometer (XRD, Rigaku D/max-II, Japan) using Cu Kα target at 40 kV and 100 mA ($\lambda = 0.154$ nm) with 2θ scan range from 1 to 15°. Transmission electron microscopy (TEM) analysis was carried out on a TECNAI G^{2}20 transmission electron microscope (FEI Company, USA) at an acceleration voltage of 200 kV. Ultrathin sections of the samples were prepared using a Leica Ultracut UCT with EMFCS cryo-attachment at −120 °C. The cross-sections with the thickness of 50 nm were obtained by using a diamond knife. ^{1}H NMR spectrum was recorded on a DRX 400 NMR spectrometer (Bruker, Switzerland) with 400 MHz at 25 °C. The spinning speed, pulse delay and total numbers of scans were 20 Hz, 15 s and

128, respectively. The sample was dissolved in deuterated chloroform ($CDCl_3$) to prepare the solution with concentration of 150 mg/mL. Differential scanning calorimetry (DSC) was performed on a DSC model 2910 (DSC, TA, USA) at a heating rate of 10 °C/min from −150 to 100 °C under nitrogen atmosphere, and all samples were annealed at 150 °C for 4 min before testing. Thermogravimetric analysis (TGA) measurement was performed with a TGA 2050 thermogravimetric analyzer (TA, USA). Samples were heated to 600 °C at a heating rate of 20 °C/min under nitrogen atmosphere. The mechanical properties of the vulcanized and unvulcanized sheets were measured by an electron tensile tester (AG-20KNG Shimadzu, Japan) according to the standard method (GB/T 528, China). The tensile rate was 500 and 100 mm/min for the vulcanized and unvulcanized sheets, respectively. The values of measurement were an average from five samples.

3. Result and discussion

3.1. Effect of OMMT on copolymerization

Dependence of conversion on reaction time of styrene–butadiene copolymerization with different OMMT contents is shown in Fig. 1. When the amount of OMMT is lower than 3 wt %, the curves of S-25M1 and S-25M3 are close to that of SB, indicating no obvious effect of OMMT on the copolymerization. However, when the OMMT content reaches to 4 wt %, the reaction rate decreases. The result indicates that the addition of OMMT does not change the kinetics of copolymerization on the whole, when its content is lower than 3 wt %. Dependence of the SBR composition with different OMMT contents on the conversion is shown in Fig. 2. The result indicates that the dependences of polymer composition on the total conversion of styrene and butadiene monomers in the nanocomposites are similar to that of SBR without OMMT. Namely, the addition of

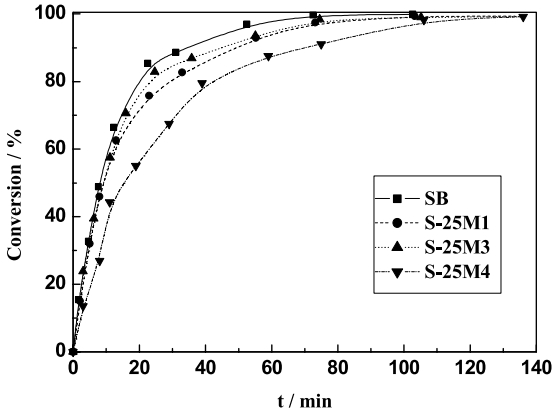

Fig. 1. Dependence of conversion on reaction time of the styrene–butadiene copolymerization with different OMMT contents.

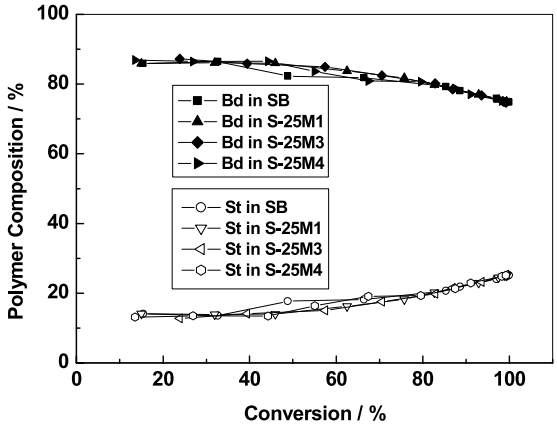

Fig. 2. Dependence of the SBR composition with different OMMT contents on the conversion.

OMMT does not change basically the composition of copolymers.

The number-average molecular weight (M_n), weight-average molecular weight (M_w) and polydispersity index (M_w/M_n) determined by GPC are summarized in Table 1. In view of the results, the M_n values of all samples are basically consistent with designed value (1.5×10^5). It is well known that M_n is defined as the total weight of all the macromolecules divided by the total number of moles present, which is highly sensitive to the presence of a small number fraction of low-molecular weight macromolecules. If the living chains were terminated significantly during the copolymerization, the low-molecular weight macromolecules would occur, and the value of M_n should decrease. So the addition of OMMT does not affect the living copolymerization on the whole, when its content is below 4 wt %. Interestingly, the addition of OMMT results in an increase of M_w/M_n and M_w, as shown in Table 1. It is noted that M_w is highly sensitive to the presence of small amounts by weight of high-molecular weight fraction. This result indicates that the introduction of OMMT has caused a higher polydispersity and an increase of M_w. It can be attributed that the OMMT affects in some way to the living chains by combination or transference and physical cross-linking between the SBR chains and a few of small particle OMMT (small particles) as junction, leading to occurrence of small amounts of high-molecular weight macromolecules.

The ^{1}H NMR spectra of the SB and S-25M3 samples are shown in Fig. 3. Usually, the resonance peak of the *ortho*

Table 1
The values of M_n, M_w, and M_w/M_n of SB and SBR/MMT nanocomposites

Sample	$M_n\times10^{-5}$	$M_w\times10^{-5}$	M_w/M_n
SB	1.47	1.58	1.07
S-25M1	1.48	2.01	1.35
S-25M2	1.43	1.95	1.37
S-25M2.5	1.54	1.81	1.18
S-25M3	1.48	2.33	1.57
S-25M4	1.74	2.22	1.27

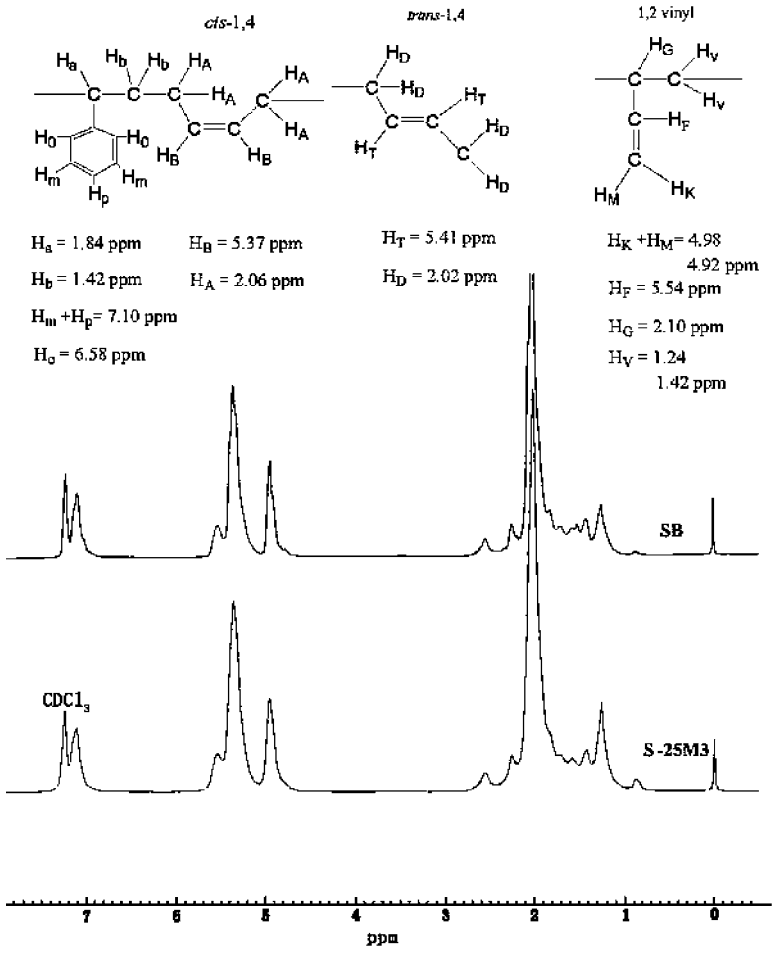

Fig. 3. The ^{1}H NMR spectra of the SB and S-25M3 samples.

proton (H_o) appears at 6.58 ppm, which is the characteristic of block styrene sequences. However, in the spectra of the SB and S-25M3 samples the characteristic peak is not observed, indicating that styrene in the samples incorporates in random way. This further reveals that the addition of OMMT has not changed almost on the randomness of the styrene–butadiene copolymer. The contents of 1,2-polybutadiene (1,2-PB), 1,4-polybutadiene (1,4-PB) and styrene have been analyzed according to the literature [26], and the data are listed in Table 2. The calculated proportion of monomers in the copolymers is in good agreement with the actually added monomer ratio. The 1,2-PB% and 1,4-PB% components of copolymer in the nanocomposites hardly change, compared with that of the SB sample. Therefore, the addition of OMMT (1–4 wt %) does affect the microstructure of the copolymer on the whole.

Table 2
The microstructure of the SB and SBR/MMT nanocomposites

Sample	$St_{non\text{-}block}$ (wt %)	1,2-PB (wt %)	1,4-PB (wt %)
SB	25.8	22.3	51.9
S-25M1	22.8	21.0	55.2
S-25M2	26.3	21.6	52.1
S-25M2.5	24.2	22.5	53.3
S-25M3	23.1	22.7	54.2
S-25M4	24.8	22.5	52.8

3.2. Structure of SBR/MMT

The TEM images of polymers/MMT composites containing styrene from 0 to 100% are shown in Fig. 4. The image of the composite S-0M3 without styrene displays clay tactoids, in which the polymer chains hardly intercalate into clay layers. With an increase of the styrene content, the samples (such as S-10M3, S-25M3, S-40M3, S-60M3 and S-100M3) exhibit a completely exfoliated structure, where the silicate layers are exfoliated and dispersed uniformly in the copolymer matrix. These results indicate that styrene plays an important role in the improvement of the exfoliated clay structure of the SBR/MMT nanocomposite. When styrene content is more than 25%, the completely exfoliated nanocomposites can be observed. As a result of the electron withdrawing effect, benzene ring has high electron cloud density. So the styrene molecules have relatively stronger polarity and more easily enter into the galleries between silicate layers than butadiene and cyclohexane molecules.

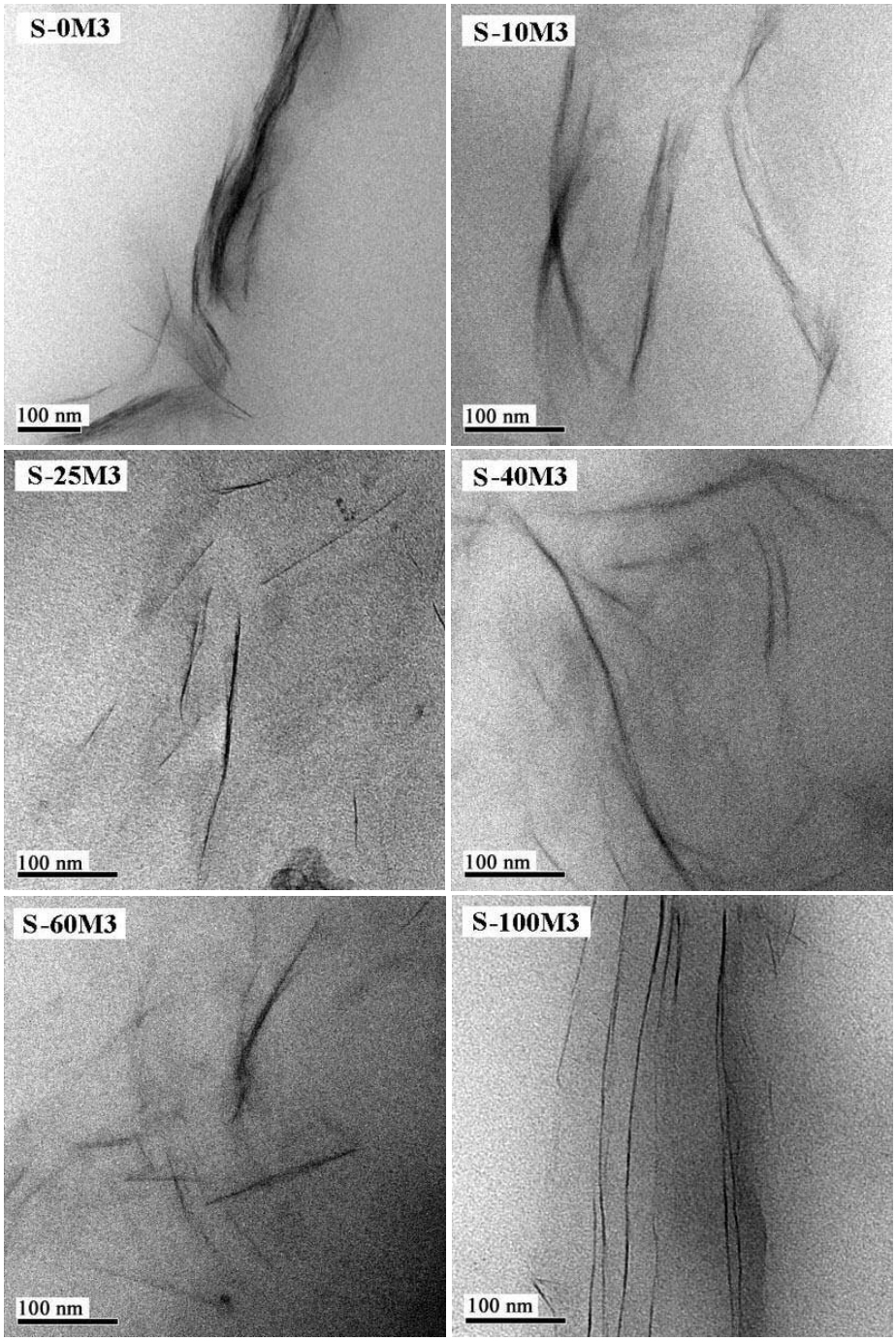

Fig. 4. TEM images of polymers/MMT composites with different styrene contents and 3 wt % OMMT.

Then the expanded galleries between layers as a result of the entering of styrene can accommodate more monomers and solvent molecules to assure the randomness of this copolymer. The XRD diffraction patterns of the OMMT and polymers/MMT composites containing different styrene contents from 0 to 100% are shown in Fig. 5. The d_{001} spacings were calculated on the basis of Bragg's law [$d_{001} = \lambda/(2 \sin \theta)$] at peak position, where d_{001}, θ and λ are the interplanar distance of (001) reflection plane, the diffraction angle and the wavelength, respectively. The diffraction peak of the (001) plane of OMMT lies at 2.46°, and the corresponding distance between the adjacent layers is 3.59 nm. For S-0M3, the diffraction peak position hardly changes, indicating that the polymer chains do not insert into the OMMT galleries. For others containing styrene (more than 10 wt %), the characteristic peak of OMMT all disappears, indicating a strong interaction between copolymer and OMMT, leading to the exfoliated structures. The results are consistent with that of TEM, and further confirm the important effect of styrene on exfoliation of OMMT.

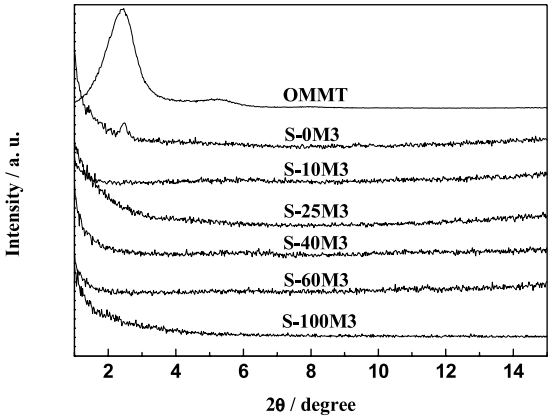

Fig. 5. X-ray diffraction patterns of the OMMT and polymers/MMT composites with different styrene contents and 3 wt % OMMT.

Thus the ratio of 25/75 of styrene to butadiene has been selected to use for the following studies.

TEM images of the S-25M3, S-25M1 and S-25M4 nanocomposites are shown in Figs. 4 and 6. All images show exfoliated structure rather than micronsized clay tactoids. The OMMT layers in the nanocomposites disperse uniformly as monolayers or 2–3 layer stacks in the copolymer matrix. The XRD diffraction patterns of the OMMT and SBR/MMT nanocomposites with different OMMT contents are shown in Fig. 7. There is no characteristic peak of OMMT in the XRD patterns for all sheets of the SBR/MMT nanocomposites. This result further confirms that the OMMT layers have been exfoliated, leading to the destruction of the MMT crystallite as a result of the strong interaction between OMMT and the styrene–butadiene copolymer.

3.3. Effect of OMMT content on properties

The DSC curves of the SB and SBR/MMT nanocomposites are shown in Fig. 8. An endotherm of SB exists at −56.20 °C, corresponding to the T_g of SB. All SBR/MMT nanocomposites show higher T_g than SB. With an increase of the OMMT amount the T_g of SBR/MMT increases slightly. This can be explained that strong interaction between OMMT and copolymer chains prevents the segmental motion of the macromolecules. From TGA and derivative thermogravimetric (DTG) curves of the SB and SBR/MMT nanocomposites, the onset decomposition temperatures (T_{d1}) by TGA and peak temperatures (T_{d2}) by DTG of the samples are listed in Table 3. The T_{d1} values of the nanocomposites are higher than that of SB, and increase with OMMT content, except for S-25M4. Especially, T_{d1} of S-25M3 shifts to a higher temperature by 18 °C compared with that of SB. The value of T_{d1} of S-25M4 is lower than that of S-25M2.5 and S-25M3. This can be attributed to the slight phase separation with further introduction of OMMT [27]. The DTG results can more clearly illustrate the difference in thermal decomposition behavior of all samples. The T_{d2} values of S-25M2.5 and S-25M3 increase by about 24 °C, compared with that of SB. The results above indicate that the thermal stability of the SBR/MMT nanocomposites is obviously improved with the addition of OMMT.

Fig. 9 illustrates the effect of the OMMT amount on the mechanical properties of the SBR/MMT nanocomposites, which have been vulcanized before tensile testing. The tensile strength (σ_b) of the SBR/MMT nanocomposites increases with an increase of OMMT, when the OMMT content exceeds 2.5 wt %. Moreover, the elongation at break (ε_b) is improved also with the addition of OMMT. When the content of OMMT reaches to 3 wt %, the ε_b value of S-25M3 increases by 34%, compared with that of SB. It is noted that OMMT plays a role in the simultaneous enhancement of σ_b and ε_b of the sheets S-25M2.5, S-25M3 and S-25M4. This suggests a presence of strong interaction between two kinds of substances and part of network structure in the material [28]. In this case, the exfoliated OMMT layers combined with intercalated agent

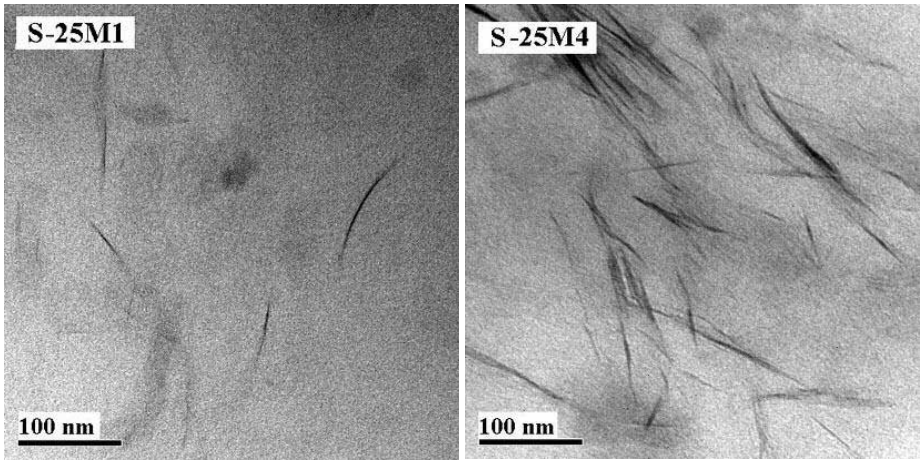

Fig. 6. TEM images of the S-25M1 and S-25M4 nanocomposites.

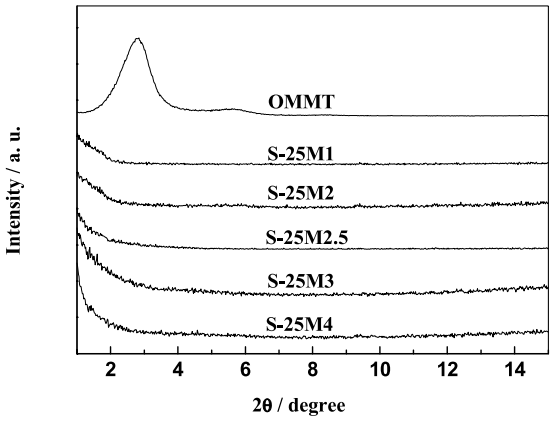

Fig. 7. X-ray diffraction patterns of the OMMT and SBR/MMT nanocomposites with different OMMT contents.

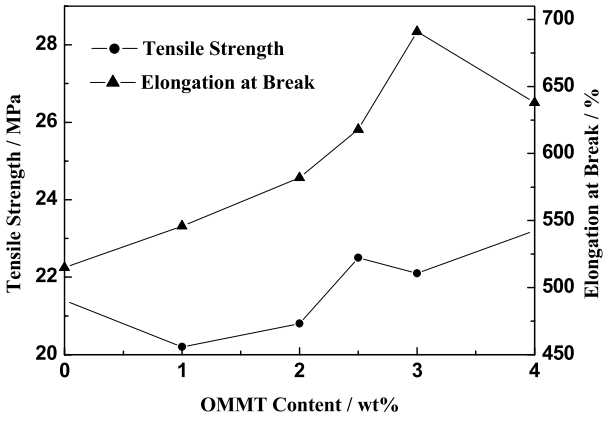

Fig. 9. Effect of OMMT content on the mechanical properties of the SBR/MMT nanocomposites.

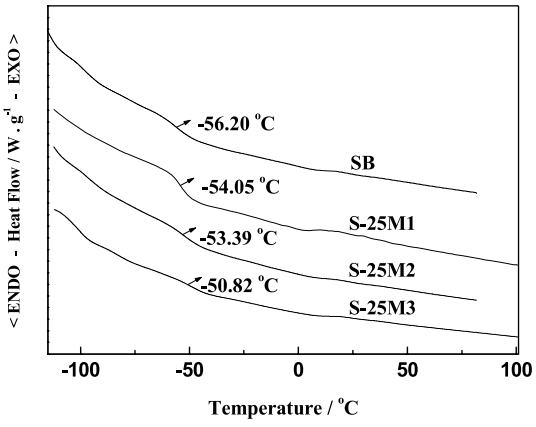

Fig. 8. DSC curves of the SB and SBR/MMT nanocomposites with different OMMT contents.

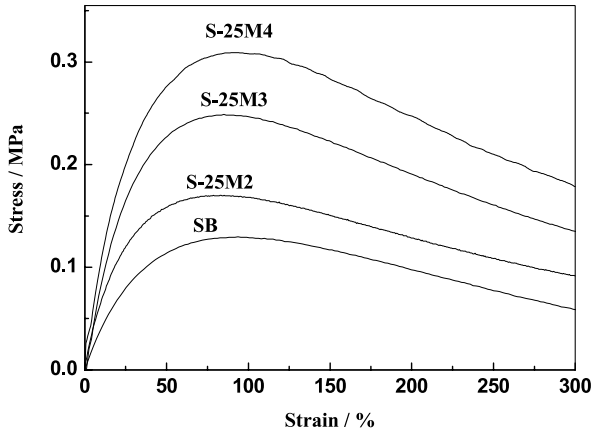

Fig. 10. Strain-stress curves of the sheets before vulcanization.

easily interact with copolymer chains to form a physical cross-linking, in which OMMT acts as a physical cross-linking junction. The relatively high values of M_w of the nanocomposites support the deduction, namely a small amount of high-molecular weight macromolecules has occurred as a result of the combination and physical cross-linking in SBR/MMT. To better understand the interaction between OMMT and the SBR copolymer, a tensile testing for the samples without vulcanization was carried out. The strain–stress curves of SB, S-25M2, S-25M3 and S-25M4 are shown in Fig. 10. The σ_b values of nanocomposites are significantly higher than that of SB, and increase with the increasing of OMMT content. The result further confirms that the strong interaction has occurred between OMMT layers and the copolymer chains, owning to the junction of OMMT in the composites.

On the basis of the information from GPC, TEM, XRD, DSC, TGA and tensile testing, a schema describing the formation and structure of the exfoliated nanocomposite is presented in Fig. 11. When styrene, butadiene, cyclohexane and OMMT have been mixed, the OMMT layers are surrounded with small molecules as shown in Fig. 11a. As a result of the electron withdrawing effect of benzene ring, the styrene molecules having relatively stronger polarity enter at the first into the galleries between silicate layers to expand the distance between OMMT layers (Fig. 11b). Then butadiene and cyclohexane molecules enter into the expanded galleries (Fig. 11c). After copolymerization a completely exfoliated nanocomposite containing 25% styrene occurs. Thus the OMMT layers are exfoliated and dispersed randomly in the copolymer matrix, which have been confirmed as shown in Figs. 6 and 7. The exfoliated layers combined with intercalated agent have strong

Table 3
The T_{d1} and T_{d2} of the SB and SBR/MMT nanocomposites

Sample	SB	S-25M1	S-25M2	S-25M2.5	S-25M3	S-25M4
T_{d1} (°C)	384.1	385.8	393.5	399.6	402.8	394.5
T_{d2} (°C)	431.9	442.7	454.4	456.3	454.4	451.4

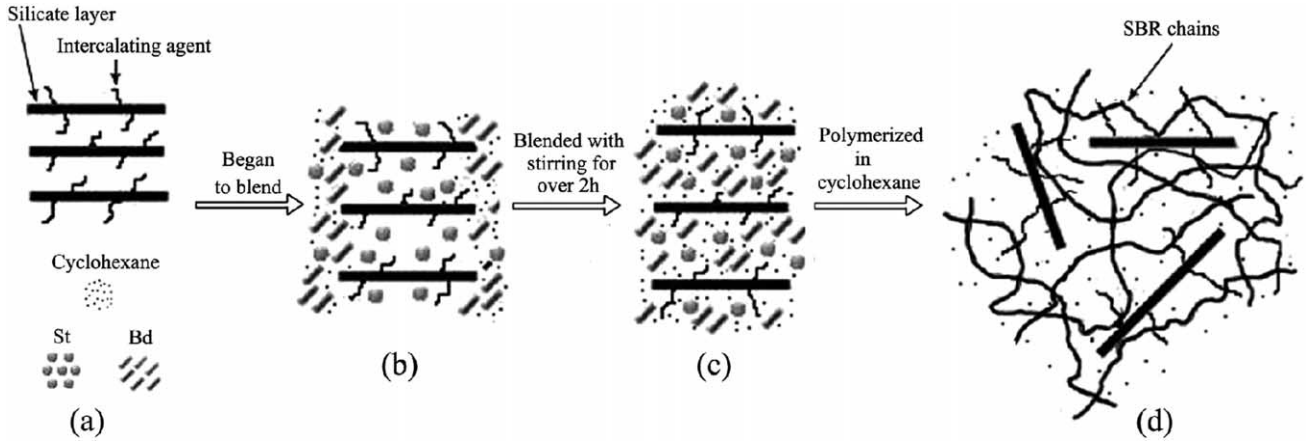

Fig. 11. Schematic formation process and the physical cross-linking network of the exfoliated SBR/MMT nanocomposite.

interaction with copolymer chains to form a cross-linking (Fig. 11d), leading to the simultaneous enhancement of σ_b and ε_b of the nanocomposites containing 2.5–4 wt % OMMT. The higher values of M_w, T_g, σ_b and ε_b of the SBR/MMT nanocomposites than those of SB support the schematic structure.

4. Conclusion

SBR/MMT nanocomposites were successfully prepared by in situ living anionic polymerization from styrene, butadiene and OMMT. When OMMT content was below 3 wt %. The addition of OMMT did not affect the living anionic copolymerization and the microstructures of the nanocomposites on the whole. Interestingly, the introduction of OMMT did not change almost the number-average molecular weight of SBR in the nanocomposites, namely absence of low-molecular weight fraction caused by the obvious termination of the living chains. However, the weight-average molecular weight and polydispersity index of SBR in the nanocomposites increased, compared with pure SBR, indicating a presence of small amounts of high-molecular weight macromolecules. The results from transmission electron microscopy and X-ray diffraction revealed that styrene played an important role in the expanding of the OMMT layers. When styrene content was more than 25 wt %, an completely exfoliated SBR/MMT nanocomposite formed. The completely exfoliated nanocomposites containing 2.5–4 wt % OMMT exhibited higher glass-transition temperature, thermal stability and mechanical properties than those of pure SBR. The DSC result showed that strong interaction existed between the SBR chains and OMMT, resulting in excellent thermal and mechanical properties of the SBR/MMT nanocomposites.

Acknowledgements

This work was supported by grants from the Institute of Chemistry, Chinese Academy of Sciences.

References

[1] Giannelis EP. Adv Mater 1996;8:29.
[2] Chen T, Tien Y, Wei K. Polymer 2000;42:1345.
[3] Usuki A, Tukigase A, Kato M. Polymer 2002;43:2185.
[4] Fu X, Qutubuddin S. Polymer 2001;42:807.
[5] Zhang W, Chen D, Zhao Q, Fang Y. Polymer 2003;44:7953.
[6] Chang J, An Y. J Polym Sci: Part B: Polym Phys 2002;40:670.
[7] Chang J, An Y, Sur G. J Polym Sci: Part B: Polym Phys 2003;41:94.
[8] Liu Y, Wu C, Chiu Y, Ho W. J Polym Sci: Part A: Polym Chem 2003; 41:2354.
[9] Lan T, Kaviratna PD, Pinnavaia TJ. Chem Mater 1995;7:2144.
[10] Yoon JT, Jo WH, Lee MS, Ko MB. Polymer 2001;42:329.
[11] Vaia RA, Ishii H, Giannelis EP. Chem Mater 1993;5:1694.
[12] Vaia RA, Jandt KD, Kramer EJ, Giannelis EP. Macromolecues 1995; 28:8080.
[13] Hackett E, Manias E, Giannelis EP. Chem Mater 2000;12:2161.
[14] Bujdak J, Hackett E, Giannelis EP. Chem Mater 2000;12:2168.
[15] Burnside SD, Giannelis EP. Chem Mater 1995;7:1597.
[16] Joly S, Garnaud G, Ollitrault R, Bokobza L, Mark J. Chem Mater 2002;14:4202.
[17] Kader MA, Nah C. Polymer 2004;45:2237.
[18] Arroyo M, Lopez-Manchado MA, Herrero B. Polymer 2003;44:2447.
[19] Brown MJ, Curliss D, Vaia RA. Chem Mater 2000;12:3376.
[20] Tjong SC, Meng YZ, Hay AS. Chem Mater 2002;14:44.
[21] Fornes TD, Hunter DL, Paul DR. Macromolecules 2004;37:1793.
[22] Choi YS, Ham HT, Chung IJ. Chem Mater 2004;16:2522.
[23] Mousa A, Karger-Kocsis J. Macromol Mater Eng 2001;286:260.
[24] Inoue S, Aida T, Kroschwitz JI. Encyclopedia of polymer science and engineering. New York: Wiley; 1987.
[25] Gilman H, Haubein AH. J Am Chem Soc 1944;66:1515.
[26] Sardelist K, Michels HJ, Allen G. Polymer 1984;25:1011.
[27] Ruan D, Zhang L, Zhang Z, Xia X. J Polym Sci: Part B: Polym Phys 2004;42:367.
[28] Huang J, Zhang L. Polymer 2002;43:2287.